

# The Effect of Chemical Modification of the Surface by Oxysilanes on Changes in the Structural and Phase States of Highly Porous Aluminum Oxyhydroxides at Annealing up to 1200°C

A. N. Khodan<sup>a, \*</sup>, A. V. Bykov<sup>b</sup>, and M. R. Kiselev<sup>b</sup>

<sup>a</sup> *Frumkin Institute of Physical Chemistry and Electrochemistry, Russian Academy of Sciences, Moscow, 199071 Russia*

<sup>b</sup> *Moscow State University, Moscow, 119899 Russia*

\**e-mail: anatole.khodan@gmail.com*

Received October 26, 2021; revised September 4, 2022; accepted September 21, 2022

**Abstract**—Changes in the composition and physicochemical properties of porous monolithic 3D nanostructures of aluminum oxyhydroxides (porous monolithic aluminum oxides, PMAO) chemically modified in methyltrimethoxysilane vapors have been studied by thermal-analysis methods. The conditions of formation and compositions of organosilicon compounds on the PMAO surface have been determined, a high degree of hydrolysis (91%) of the alkoxy groups of the modifier during chemisorption has been confirmed. The dependence of the composition of the porous nanocomposite structure ( $\text{Al}_2\text{O}_3\text{--SiO}_2$ ) on the conditions of chemical and thermal treatment has been investigated. General changes in the chemical composition of the nanocomposite when using different annealing times in the range from 100 to 1200°C has been described.

**Keywords:** nanomaterial, 3D nanostructure, aluminum hydroxides, chemical modification of the surface, thermal analysis

**DOI:** 10.1134/S2070205123700193

## INTRODUCTION

The study of the structure and physicochemical properties of porous media and 3D nanocomposites comprises an important task of modern materials science. The properties of nanocomposite media can differ significantly from those of both bulk materials and individual nanoparticles forming a nanocomposite material, which opens up new opportunities for creating materials with certain dielectric, magnetic, and optical properties depending on the degree of ordering, size, shape, chemical, and phase composition of nanoparticles [1]. One should especially note that the development of the technology of new nanomaterials and nanocomposites based on porous structures opens up additional opportunities for creating optical media with controlled properties for the terahertz range.

In the present work, we investigated 3D nanomaterials synthesized using an original technology [2–4], the products of which were monolithic highly porous structures that represented a spatial 3D grid of aluminum hydroxide nanofibrils of a diameter of  $6 \pm 2$  nm and an average length of 100–300 nm. Highly porous monolithic blocks of the material based on nanostructured aluminum oxyhydroxides (PMAO) synthesized recently normally have a volume of up to 1 dm<sup>3</sup> and a constant cross-sectional area, which is determined by the size and shape of the metallic Al plate, whereas the

height depends on the synthesis time: at room temperature, the growth rate of PMAO is  $\approx 1$  cm/h. In terms of physical and chemical properties, PMAO materials are very similar to aerogels, but differ from them fundamentally in the method of production: the surface of a liquid metal alloy containing aluminum is oxidized in one stage at room temperature in a humid air atmosphere. PMAO materials retain their solidity during annealing up to 1700°C and above, but the linear dimensions of the samples decrease isotropically, while their physical properties change significantly: density from  $\approx 0.02$  to  $\leq 3$  g/cm<sup>3</sup>, open porosity from 99.3 to 25%, specific surface area from 300 to 1 m<sup>2</sup>/g, and the phase composition from amorphous  $\text{Al}_2\text{O}_3 \cdot 4\text{H}_2\text{O}$  to  $\gamma$ -,  $\theta$ -, and  $\alpha$ - $\text{Al}_2\text{O}_3$  [2–6].

One should mention that the prospects of using PMAO-based materials for terahertz optics are particularly determined by the possibility of optimizing an important parameter of the complex permittivity of a medium. Controlling the 3D structure parameters and changes in the chemical composition of PMAO allows changing the dielectric, magnetic, and optical properties of a material. High and completely open porosity of PMAO materials makes it possible both to chemically modify both the surface of nanofibrils and fill the free space in the 3D nanostructure with nanoparticles using liquid and gaseous media [7–12]. Treatment of

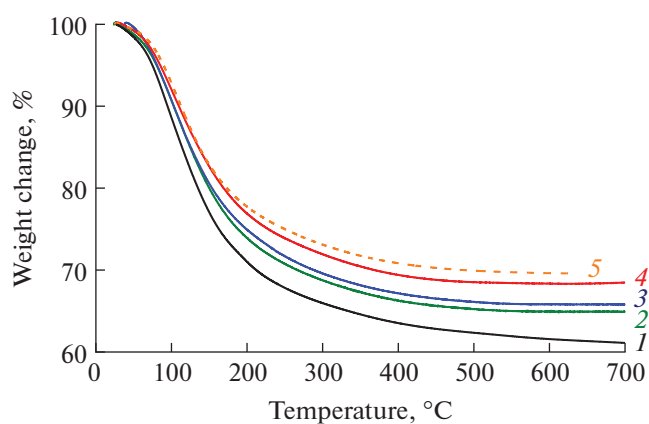


**Fig. 1.** Results of TGA studies of the samples: (1) PMAO, (2) PMAO-M(2), (3) PMAO-M(3), (4) PMAO-M(4), and (5) PMAO-M(7).

the nanofibrils' surface with organosilicon compounds (tetraethoxysilane (TEOS), trimethylethoxysilane (TMES), and methyltrimethoxysilane (MTMS)) with subsequent annealing up to 450°C is a simple and efficient method to deposit a thin layer of SiO<sub>2</sub> on the surface of nanofibrils [9–12]. The presence of even a monomolecular layer of SiO<sub>2</sub> noticeably affects the diffusion mass transfer in the surface layer of nanofibrils of the PMAO–SiO<sub>2</sub> composite, which, when the samples are annealed up to ≤800°C, results in a significant difference in the properties of the original and modified nanomaterials, namely, the 3D structure parameters, bulk density, morphology of nanofibrils, and kinetics of the phase transition of amorphous Al<sub>2</sub>O<sub>3</sub>·*n*H<sub>2</sub>O into the γ-phase of Al<sub>2</sub>O<sub>3</sub> [11, 12].

PMAO materials remain monolithic during annealing up to 1700°C and above; however, the linear dimensions of the samples decrease isotropically, while their physical properties change significantly: density from ≈0.02 to ≤3 g/cm<sup>3</sup>, open porosity from 99.3 to 25%, specific surface area from 300 to 1 m<sup>2</sup>/g, and structural-phase state from amorphous oxyhydroxide Al<sub>2</sub>O<sub>3</sub>·*n*H<sub>2</sub>O, where *n* ≈ 3.4–4.6, to crystalline oxides, γ-, θ-, and α-Al<sub>2</sub>O<sub>3</sub> [2–6].

The objective of the present work was to study the effect of the processing time in MTMS vapors on the chemical composition and evolution of the structural parameters of PMAO–SiO<sub>2</sub> nanocomposites (hereinafter, PMAO-M) at thermal treatment up to 1200°C. Particular attention was paid to the water content in the nanomaterials as the main factor causing losses in the terahertz range.

## EXPERIMENTAL

Monolithic PMAO samples were grown on the surface of a thin layer of mercury (several microns) deposited on the surface of an Al plate of a thickness of

0.5 mm. The samples were grown in a climate chamber with a controlled air atmosphere at a constant temperature of 25°C and humidity of 70%. Under these conditions, a monolithic 3D nanostructure formed and grew strictly normally to the surface of the Al plate. The PMAO growth rate was ~1 cm/h [2–4].

Chemical modification of the surface of the PMAO samples was carried out at room temperature in saturating MTMS vapors, the processing time was 2, 3, 4, and 7 hours. Both the initial PMAO samples and the PMAO-M samples were processed in MTMS vapors for 4 h and, then, annealed in a muffle furnace at fixed temperatures in the range from 100 to 1200°C for 4 h. After each stage of the processing, the samples of PMAO and PMAO-M were weighed, their linear dimensions were measured, and the changes in mass and volume density were estimated.

The PMAO and PMAO-M samples were studied by thermal analysis (TA) methods in dynamic and modulation modes in an argon medium using DSC-Q100 and TGA-Q500 devices (TA Instruments, United States), as well as in a nitrogen atmosphere using a TGA-Q50 device (TA Instruments, United States) fitted with a Nicolet iS 10 IR Fourier spectrometer (Thermo Fisher Scientific, United States).

## RESULTS AND DISCUSSION

Thermal treatment of the PMAO and PMAO-M samples results in an isotropic decrease in their linear dimensions, increase of the volume density, and changes of the structural-phase state of the fibril material from amorphous to crystalline. Along with increasing density, their mechanical strength also increases.

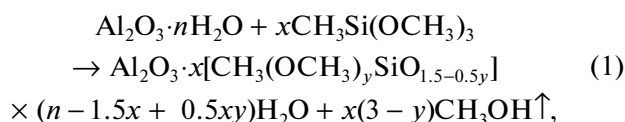
The thermogram of the unprocessed PMAO sample is shown in Fig. 1. The mass-loss curve has two characteristic sections: a low-temperature one from ~20 to 250°C, where losses reach ~30%, and a high-temperature one from 250 to 700°C, where the maximum mass loss of the sample does not exceed 15%. In earlier-published works [4, 6], the composition of PMAO was described as Al<sub>2</sub>O<sub>3</sub>·*n*H<sub>2</sub>O, where *n* = 3.6–4.2. As for the PMAO sample grown at 25°C and 70% humidity, we obtained the following value: *n* = 3.59 ± 0.3.

Figure 1 also shows thermograms of PMAO-M(X) samples that were chemically treated with MTMS vapors, where X is the duration of treatment in hours. As follows from comparing the mass-loss curves, the main difference between the PMAO and PMAO-M(X) samples was observed for the relative total mass loss: the longer the exposure time in MTMS vapors, the less the mass loss at annealing (Table 1). As can be concluded from the results given in Table 1 and Fig. 2, (1) treatment of the samples in MTMS vapors at room temperature leads to an increase of the mass of the PMAO samples, whereas the maximum saturation of the surface with hydrolysis products is achieved in 4 h,

**Table 1.** Results of TGA studies of PMAO-M(X) samples in the temperature range of 20–700°C, where  $m/m_0$  is a relative change in the mass of the samples as a result of treatment with MTMS,  $\Delta m$  is a relative increase in the mass of samples treated with MTMS vapors, and  $\Delta\omega$  is a relative total mass loss when the samples are heated to  $T_{\max} = 700^\circ\text{C}$

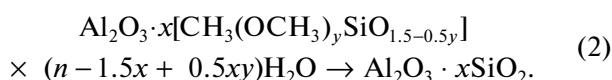
Sample	$m/m_0$	$\Delta m, \%$	$\Delta\omega, \%$	$x$	$y$
PMAO	—	—	40.52	—	—
PMAO-M(2)	1.0982	9.8208	35.08	$0.36 \pm 0.06$	$0.23 \pm 0.14$
PMAO-M(3)	1.0990	9.8947	34.10	$0.41 \pm 0.16$	$0.25 \pm 0.08$
PMAO-M(4)	1.1363	13.6313	31.64	$0.46 \pm 0.04$	$0.27 \pm 0.09$
PMAO-M(7)	1.0888	8.8797	30.38	$0.41 \pm 0.07$	$0.16 \pm 0.07$

and (2) the process of hydrolysis of MTMS is determined by its interaction with hydroxyl groups and adsorbed water on the surface of PMAO. This process reduces the water content in the samples; however, the total mass of the PMAO-M(X) samples increases due to the deposition of hydrolysis products, which can be described by the following reaction equation:



where  $x$  is the number of moles of MTMS adsorbed on the surface per 1 mol of  $\text{Al}_2\text{O}_3$  and  $y$  is the average fraction of nonhydrolyzed methoxy groups in MTMS molecules.

During the TGA process, the PMAO-M(X) samples were heated up to  $T_{\max} = 700^\circ\text{C}$ , which led to the complete decomposition of hydrolysis products with the formation of a thin layer of  $\text{SiO}_2$  on the surface of the nanocomposite structure,  $\text{Al}_2\text{O}_3 \cdot x\text{SiO}_2$ :



From the TGA data and measurements of relative mass changes during the annealing of the PMAO and PMAO-M(X) samples, parameters  $x$  and  $y$  in equation (1) (Table 1) were estimated, which enabled us to establish almost complete (~91%) hydrolysis of methoxy groups on the surface; here, the molar content of Si in the material was from 15 to 25% per mol Al (Fig. 2). For comparison, the authors of [12] performed chemical modification of PMAO using TEOS and obtained molar ratios Si/Al from 5 to 25%, depending on the processing time. The obtained identical maximum values of the Si content confirmed that the model describing the saturation of the PMAO surface with hydrolysis products was sound.

The proportion of the surface occupied by the adsorbate under conditions close to saturation was estimated. If we proceed from the assumption that some of the MTMS molecules adsorbed on the surface remain nonhydrolyzed, while the rest of the surface is covered with  $\text{CH}_3\text{Si}(\text{O}-)_3$ , a product of complete hydrolysis of MTMS, then the proportion of adsorbed

MTMS molecules does not exceed 9% and the residues of complete hydrolysis are equal to 91%.

To estimate the area occupied by one MTMS molecule, we assumed the value of the molar volume of the molecule as  $109.172 \text{ cm}^3/\text{mol}$ , which was calculated using the Gaussian 09 program and quantum-chemistry calculation of the optimal structure and volume of molecules. The area occupied by the adsorbed molecule on the surface was estimated based on the assumption of that the molecule has a spherical shape. This assumption was quite justified if we considered the fact that the central Si atom in  $\text{CH}_3\text{Si}(\text{O}-)_3$  was in a tetrahedral environment. By occupied area, the residue of  $\text{CH}_3\text{Si}(\text{O}-)_3$  is virtually equal to the size of the  $\text{SiO}_2$  molecule [13], which remains on the surface as a result of annealing. The thickness of the  $\text{SiO}_2$  layer on the surface of the 3D  $\text{Al}_2\text{O}_3\text{-SiO}_2$  nanocomposite was  $0.97 \pm 0.07$ , i.e.,  $\approx 1$  monolayer.

One should mention that the treatment of PMAO at  $T \geq 30^\circ\text{C}$  and high pressures of saturating MTMS vapors could lead to the formation of cavities of up to 1 mm in size inside the monolith, destroying the uniformity of the 3D structure. We attribute this to the formation of MTMS condensate in the volume of the

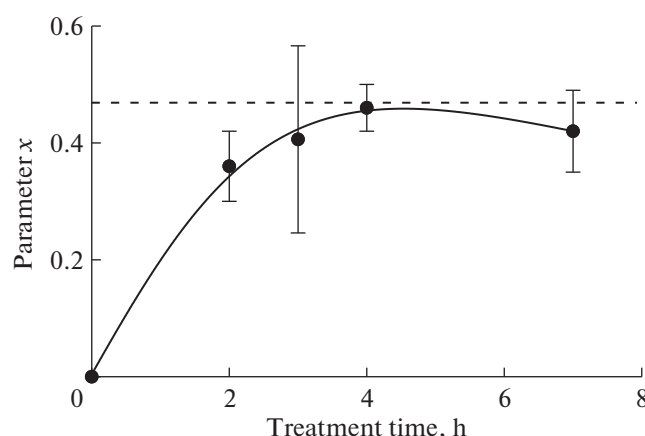


**Fig. 2.** Dependence of parameter  $x$ , which determines the Si content in the NAOM samples, on the processing time with MTMS vapors.

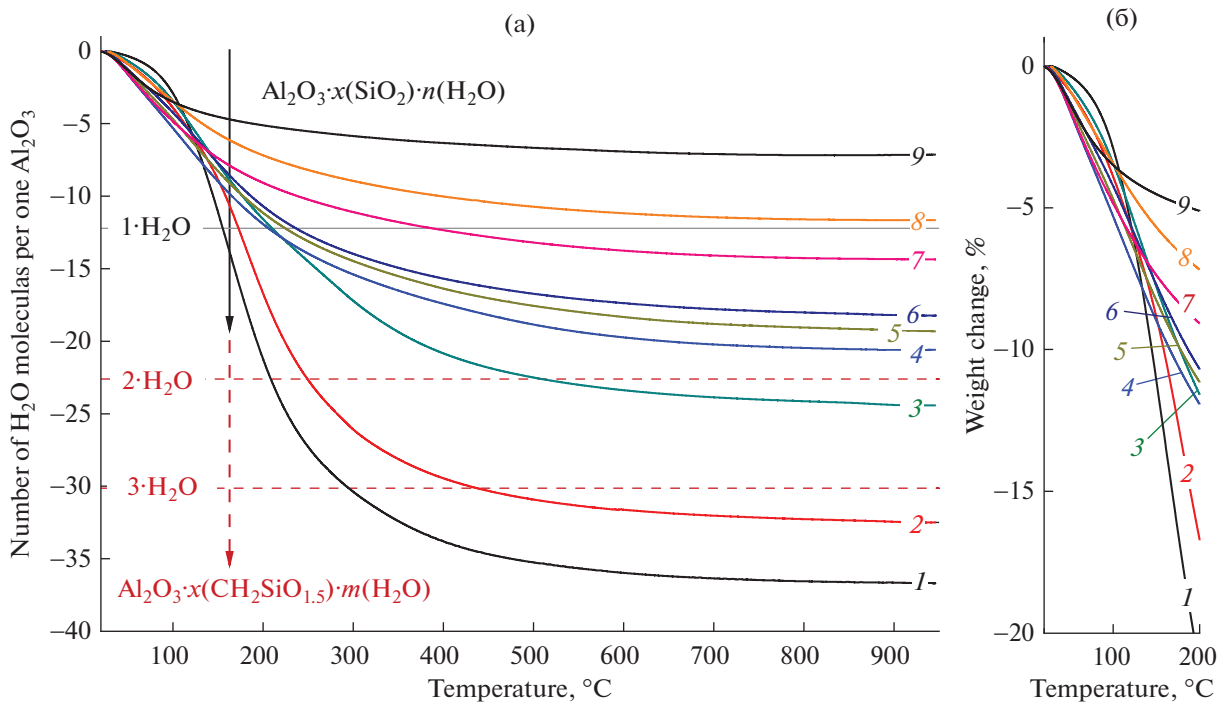


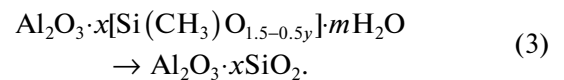
**Fig. 3.** Study of the effect of pre-annealing on the composition of PMAO-M(4) samples. (a) Changes in the relative content of H<sub>2</sub>O per Al<sub>2</sub>O<sub>3</sub> molecule after pre-annealing at temperature  $T_h$ , the composition of samples after pre-annealing is given, and  $m$  is the number of moles of H<sub>2</sub>O per 1 mol Al<sub>2</sub>O<sub>3</sub> after annealing up to  $T_{max} = 700^\circ\text{C}$ : (1) PMAO-M(4), without annealing,  $Al_2O_3 \cdot 0.46[CH_3(CH_3O)_{0.27}SiO_{1.365}] \cdot 3.84H_2O$ ; (2)  $T_h = 100^\circ\text{C}$ ,  $Al_2O_3 \cdot 0.46[CH_3(CH_3O)_{0.17}SiO_{1.415}] \cdot 3.19H_2O$ ; (3)  $T_h = 200^\circ\text{C}$ ,  $m = 2.32$ ; (4)  $T_h = 380^\circ\text{C}$ ,  $m = 1.87$ ; (5)  $T_h = 520^\circ\text{C}$ ,  $m = 1.73$ ; (6)  $T_h = 650^\circ\text{C}$ ,  $m = 1.66$ ; (7)  $T_h = 900^\circ\text{C}$ ,  $m = 1.21$ ; (8)  $T_h = 1000^\circ\text{C}$ ,  $m = 0.94$ ; and (9)  $T_h = 1200^\circ\text{C}$ ,  $m = 0.554$ . (b) Thermograms in the low temperature range of 20–200°C. Samples pre-annealed at  $T_h \geq 380^\circ\text{C}$  show a significant difference in the course of the decomposition curves of the deposited products to  $T \sim 150^\circ\text{C}$ .

3D structure and on the surface of nanofibrils, with subsequent destruction by capillary forces.

The effect of prethermal treatment on changes in the overall chemical composition was studied on the PMAO-M(4) samples, and the results are shown in Fig. 3. An increase in pre-annealing temperature  $T_h$  leads to a decrease of the total mass loss of the samples at  $T_{max} = 700^\circ\text{C}$ . To describe the evolution of the chemical composition of the samples, two temperature ranges of pre-annealing should be discerned. The first range is low-temperature,  $T_h \leq 380^\circ\text{C}$ . Under these conditions, complete hydrolysis of methoxy groups occurs and the bound water is partially removed from nanofibrils; however, methyl groups ( $CH_3-$ ) remain on the surface and the total composition of the surface layer can be described as  $Al_2O_3 \cdot x[Si(CH_3)O_{1.5-0.5y}] \cdot mH_2O$ , where  $m$  is the number of mol H<sub>2</sub>O per 1 mol Al<sub>2</sub>O<sub>3</sub>. Quantitative estimates of parameter  $m$  for the thermograms obtained at TGA with  $T_{max} = 700^\circ\text{C}$  are given in the caption to Fig. 3.

During high-temperature annealing of the samples at  $T > 400^\circ\text{C}$  and above, all the adsorbed water is removed, methyl groups are oxidized, and a layer of SiO<sub>2</sub> is formed on the surface [14]. Heating the sam-

ples up to  $800^\circ\text{C}$  and above reduces the content of structural water in nanofibrils to  $m < 0.1$  and the crystallization of the  $\gamma$ -Al<sub>2</sub>O<sub>3</sub> phase begins. At temperatures above  $1200^\circ\text{C}$ , all the structural water is completely removed and the  $\alpha$ -Al<sub>2</sub>O<sub>3</sub> phase is formed [4]:



To establish the sequence of decomposition stages of the deposited products, measurements were carried out in the modulation mode. Activation energy  $E_a$  was estimated for various stages of decomposition [15]. The activation energy for NAOM-4h (Fig. 4a) has a plateau in the range of 100–440°C corresponding to a stage of decomposition: the removal of water. In addition, there is a peak around  $\sim 450^\circ\text{C}$ , which indicates the beginning of another stage occurring simultaneously with the previous one. For the NAOM sample (Fig. 4b), a significant deviation from the constant value of  $E_a$  begins at  $\sim 300^\circ\text{C}$ . Thereafter, the dependence takes on a more complex form, the interpretation of which becomes difficult. However, on the mass loss curve at  $T \approx 850^\circ\text{C}$ , there is a step corresponding to the loss of  $\sim 1.5\%$  H<sub>2</sub>O during the phase transition of aluminum hydroxide  $\gamma$ -Al<sub>2</sub>O<sub>3</sub> [4]. Since the obtained

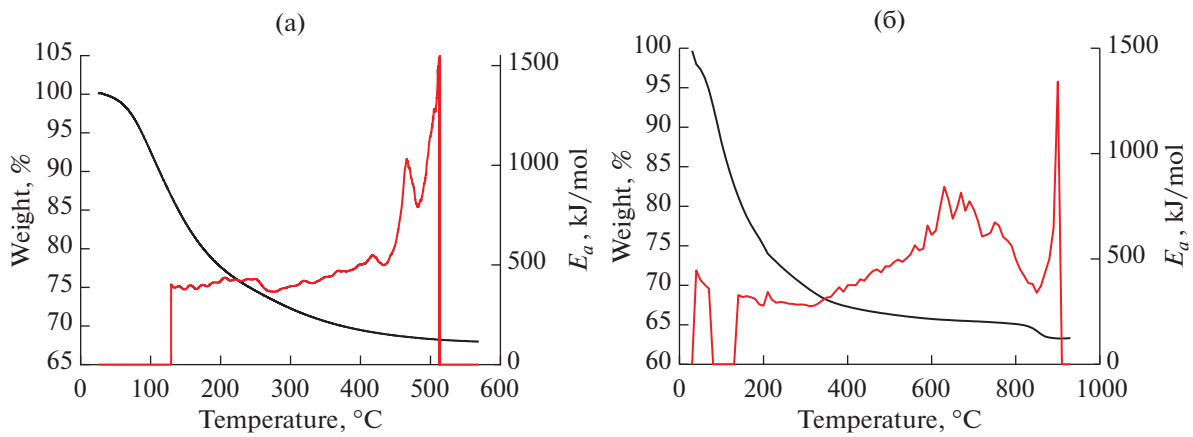


Fig. 4. TG and DTG curves obtained in the modulation mode for samples of (a) NAOM-4h and (b) NAO.

results do not allow complete separation of the stages of phase transitions, the obtained numerical values of the activation energy must be considered as estimated ones.

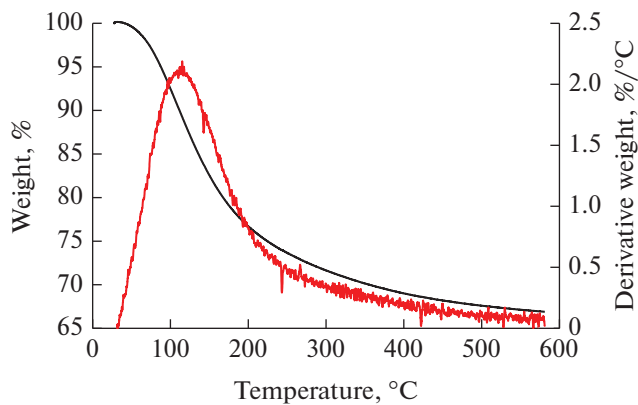


Fig. 5. DTG curve of the NAOM-2h sample.

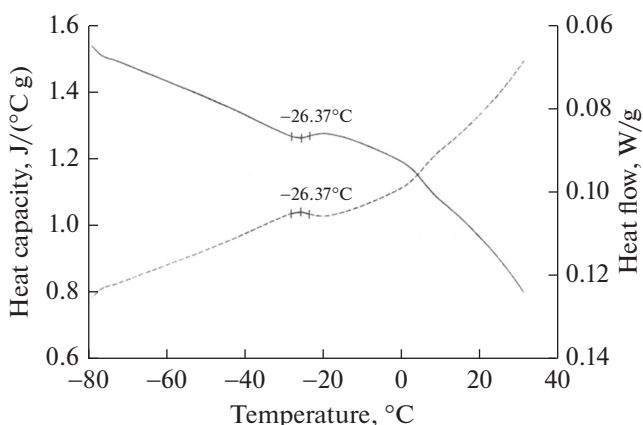


Fig. 6. DTA curves for cooling and reverse heating of the NAO sample: (1) heating curve; (2) cooling curve.

No residues of organic decomposition products were detected during annealing of the samples NAO, NAOM-2, NAOM-3, and NAOM-4 by IR-Fourier spectroscopy. This can be explained by their low content, as well as a fairly long annealing stage in the air atmosphere. The IR spectra of the samples studied do not virtually differ, while bands associated with water absorption are observed on all of them. Changes in the intensities of the bands over time correspond to the graph of differential TG curves indicating the release of water throughout the decomposition process (Fig. 5).

The DSC curves at cooling to  $T = -85^{\circ}\text{C}$  and reverse heating did not show transitions to crystallization or melting (Fig. 6). At  $T = -27^{\circ}\text{C}$ , a curve bend similar to the glass transition was observed. This fact indicates the bound state of water molecules in NAO and preventing crystallization (Fig. 6).

## CONCLUSIONS

As a result of the study, we have determined a relationship in changes in the composition and structural-phase properties of nanostructured aluminum hydroxide during its modification of methyltrimethoxysilane and heat treatment. The composition of the NAO samples has been confirmed:  $\text{Al}_2\text{O}_3 \cdot n\text{H}_2\text{O}$ , where  $n = 3.6$ . A high-temperature stage of decomposition of the material corresponding to the phase transition of aluminum hydroxide to  $\gamma\text{-Al}_2\text{O}_3$  has been detected by the modulation TGA method.

The dependence of the chemical composition of NAO nanocomposites with MTMS processing products on the holding time of NAO samples in vapors has been established. Four hours are enough to fully saturate the surface: during this time, the formation of a monomolecular layer of chemisorbate occurs. As a result of interaction with the surface, hydrolysis of methoxy groups characterized by a degree of transformation equal to 91% takes place. The composition of

NAOM samples after high- and low-temperature annealing at different temperatures has been studied.

#### FUNDING

The work was carried out as a preparatory stage for the application for participation in the project and was partially supported by the Russian Science Foundation, project no. 22-23-01011 “New Composite Materials and Protective Coatings Based on 3D Porous Corundum Structures Filled with Tungsten or Tungsten Carbides with Increased Stability in High-Energy Gas and Plasma Flows.”

#### CONFLICT OF INTEREST

The authors declare that they have no conflicts of interest.

#### REFERENCES

1. Golovan, L.A., Timoshenko, V.Yu., and Kashkarov, P.K., *Phys.-Usp.*, 2007, vol. 50, no. 6, p. 595.
2. di Costanzo, T., Fomkin, A.A., Frappart, C., Khodan, A.N., Kuznetsov, D.G., Mazerolles, L., Michel, D., Minaev, A.A., Sinitsin, V.A., and Vignes, J.-L., *Mater. Sci. Forum*, 2004, vols. 453–454, p. 315.
3. Vignes, J.-L., Frappart, C., di Costanzo, T., Rouchaud, J.-C., Mazerolles, L., and Michel, D., *J. Mater. Sci.*, 2008, vol. 43, p. 1234.
4. Khodan, A., Nguyen, T.H.N., Esaulkov, M., Kiselev, M.R., Amamra, M., Vignes, J.-L., and Kanaev, A., *J. Nanopart. Res.*, 2018, vol. 20, p. 194.
5. Karlash, A.Yu., Skryshevsky, V.A., Khodan, A.N., Kanaev, A.V., and Gayvoronsky, V.Ya., *J. Phys. D: Appl. Phys.*, 2012, vol. 45, p. 365108.
6. Khodan, A.N., Kopitsa, G.P., Yorov, Kh.E., Baranchikov, A.E., Ivanov, V.K., Feoktystov, A., and Pipich, V., *J. Surf. Invest.: X-ray, Synchrotron Neutron Tech.*, 2018, vol. 12, no. 2, p. 296.
7. Martynov, A.G., Bykov, A.V., Gorbunova, Yu.G., Khodan, A.N., and Tsivadze, A.Yu., *Prot. Met. Phys. Chem. Surf.*, 2018, vol. 54, p. 185.
8. Yorov, Kh.E., Khodan, A.N., Baranchikov, A.E., Utochnikova, V.V., Simonenko, N.P., Beltiukov, A.N., Petukhov, D.I., Kanaev, A., and Ivanov, V.K., *Microporous Mesoporous Mater.*, 2020, vol. 293, p. 109804.
9. Bouslama, M., Amamra, M.C., Jia, Z., Ben Amar, M., Chhor, K., Brinza, O., Abderrabba, M., Vignes, J.-L., and Kanaev, A., *ACS Catal.*, 2012, vol. 2, p. 1884.
10. Bouslama, M., Amamra, M.C., Brinza, O., Tieng, S., Chhor, K., Abderrabba, M., Vignes, J.-L., and Kanaev, A., *Appl. Catal., A*, 2011, vol. 402, nos. 1–2, p. 156.
11. Mukhin, V.I., Khodan, A.N., Nazarov, M.M., and Shkurinov, A.P., *Radiophys. Quantum Electron.*, 2012, vol. 54, nos. 8–9, p. 591.
12. Khatim, O., Nguyen, T.H.N., Amamra, M., Museur, L., Khodan, A.N., and Kanaev, A., *Acta Mater.*, 2014, vol. 71, p. 108.
13. Katsuki, F., Saguchi, A., Takahashi, W., and Watanabe, J., *Jpn. J. Appl. Phys.*, 2002, vol. 41, p. 4919.
14. Inoue, Y. and Takai, O., *Plasma Sources Sci. Technol.*, 1996, vol. 5, p. 339.
15. Blaine, B.L. and Hahn, B.K., *J. Therm. Anal. Calorim.*, 1998, vol. 54, p. 695.

Translated by D. Marinin

SPELL: 1. OK